Evolution of Zinc Carboxylate Species in Oil Paint Ionomers

Beerse, M.; Keune, K.; Iedema, P.; Woutersen, S.; Hermans, J.

DOI
10.1021/acsapm.0c00979
Publication date
2020
Document Version
Final published version
Published in
ACS Applied Polymer Materials

ACS APPLIED POLYMER MATERIALS

pubs.acs.org/acsapm

Article

Evolution of Zinc Carboxylate Species in Oil Paint Ionomers

Marit Beerse, Katrien Keune, Piet Iedema, Sander Woutersen, and Joen Hermans*

Cite This: *ACS Appl. Polym. Mater.* 2020, 2, 5674−5685

Read Online

ACCESS | Metrics & More | Article Recommendations | Supporting Information

ABSTRACT: Oil paint binding media are complex polymer networks that harbor populations of metal ions. Understanding of the reactivity of these metal ions, often closely linked to paint degradation, is crucial to support paintings conservation efforts. By developing a spectrum fitting approach for the analysis of Fourier transform infrared spectra, we have studied in detail how the molecular structures of zinc carboxylate species in oil paint ionomers change in the lifetime of a painting. It was found that high ZnO pigment content, humidity, and low paint viscosity all stimulate the formation of ionomeric zinc carboxylate species, while the structures (chain or oxo) adopted by those species depend on carboxylate concentration and humidity. Moreover, we found evidence for a difference in reactivity between the two structures for ionomeric zinc carboxylates toward the formation of crystalline zinc soaps. The results have yielded an abundance of information about the internal chemistry of oil paint layers and metal-containing polymers in general.

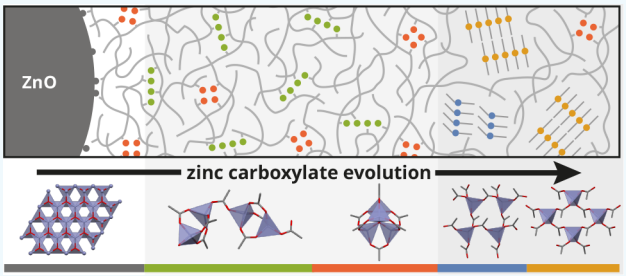

KEYWORDS: *oil paint, ionomer, zinc carboxylates, ATR-FTIR spectroscopy, humidity, peak fitting*

1. INTRODUCTION

Zinc ions play an important role in the degradation of oil paintings. In the period 1850−1950, zinc white (ZnO) was one of the most prevalent white pigments in artists' oil paints.[1] In recent years, researchers are beginning to understand how the pigment and its reaction products can be harmful to the appearance and structural integrity of oil paint layers. Oil binders in paintings cure by a radical polymerization process that involves the unsaturated fatty acid chains of the oil triglycerides and atmospheric oxygen.[2] During this initial polymerization and subsequent aging, pendant carboxylic acid groups can form as a consequence of chain scission reactions or hydrolysis of the triglyceride esters.[3,4] Zinc oxide is actively broken down by reaction with these carboxylic acids, leading to a population of zinc ions bound to pendant carboxylate groups in the oil polymer network, as illustrated in Figure 1a.[5,6] In this *ionomer* state, zinc ions have the potential to react further with saturated fatty acids to form zinc soaps, which have a tendency to separate from the polymer medium and form crystallites.[7,8] These saturated fatty acids can be part of the paint formulation as aluminum stearate additives,[1] or they can be the product of hydrolysis reactions in the polymer network, whose triglyceride monomers typically contain about 10% saturated fatty acids.[9] The formation of zinc soaps has been linked to many types of paint degradation, like delamination, paint flaking, and the appearance of disfiguring protrusions.[10−13] Given this propensity for instability, preventing or slowing down the formation of zinc soaps is generally seen as an important objective for the conservation of oil paintings that contain the zinc white pigment.

Using infrared (IR) spectroscopy, we have previously investigated the carboxylate vibration bands in oil paint polymer systems to elucidate all possible coordination environments around zinc ions in aging oil paint (Figure 1b). In the ionomer state, 2D-IR spectroscopy showed that two distinct zinc carboxylate species exist in typical zinc white oil paints: a tetranuclear oxo complex and a linear coordination chain complex.[17] After reaction with saturated fatty acids, the zinc ions can crystallize as zinc soaps in two different structures: one that optimizes zinc carboxylate coordination (type A) and one that optimizes fatty acid chain packing (type B).[18] This total of four possible coordination environments for zinc carboxylates in oil paint all have distinct asymmetric carboxylate stretch vibration (ν_a COO−Zn) features in IR spectra, as shown in Figure 1b. The highly symmetric oxo complex and type B crystalline zinc soap exhibit a single ν_a COO−Zn vibration band (around 1590 and 1538 cm^{-1}, respectively), while the lower symmetry chain complex and type A zinc soap give rise to multiple ν_a COO−Zn bands that are the result of vibrational coupling between geometrically distinct carboxylate groups. The recent structural elucidation of these four types of zinc carboxylates now makes it possible to investigate how changes in the concentrations of functional

Received: September 3, 2020
Accepted: November 16, 2020
Published: December 2, 2020

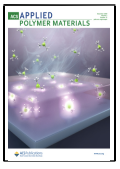

https://dx.doi.org/10.1021/acsapm.0c00979
ACS Appl. Polym. Mater. 2020, 2, 5674−5685

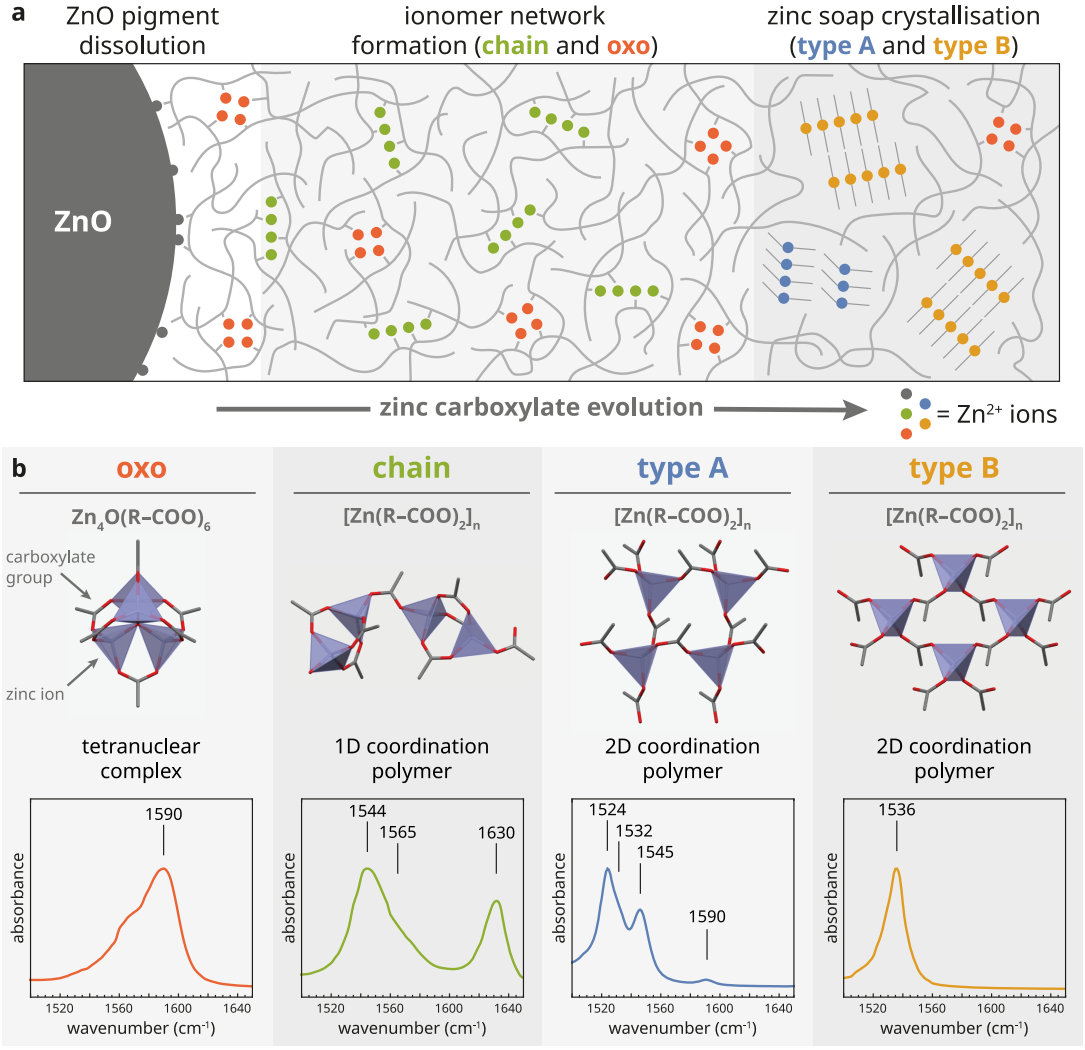

Figure 1. (a) Illustration of the different stages in the evolution of zinc carboxylates in zinc white oil paint. (b) Overview of four possible zinc carboxylate coordination geometries in zinc white oil paint and their corresponding ν_a COO−Zn features in IR spectra. Carbon atoms are gray, oxygen is red, and zinc ions are indicated with blue tetrahedra. All carbon atoms except the first beyond the carboxylate group are omitted for clarity. The indicated positions of bands in IR spectra are approximate values; band positions in oil paint samples may vary due to, for instance, disorder in coordination, variations in carboxylate backbone, and temperature. The IR spectra correspond to liquid zinc palmitate (oxo), liquid zinc palmitate (chain), zinc oleate (type A), and crystalline zinc palmitate (type B). The shoulder at 1565 cm^{-1} in the spectrum of the oxo complex is considered to be caused by an impurity, given that no band shoulders have ever been reported for oxo complexes in ionomers[14,15] or in solution.[16]

groups, polymer network connectivity, and relative humidity (RH) affect the structure of zinc carboxylates in oil paint. Moreover, we can now analyze in detail all stages in the evolution of zinc carboxylate species during oil paint drying, aging, and degradation, which can give valuable information about the local chemical conditions inside oil paint layers and the potential risks of conservation treatments.

Interestingly, the behavior of zinc ions in oil paint systems is closely related to previous research on ionomeric polymers and rubbers. Several researchers have made attempts to elucidate the structural changes in ionic aggregates upon water absorption[14,19] and have studied transformations in structure of zinc soap fillers in polymer or ionomer systems.[20−22] Comparison with the IR spectra reported by these researchers shows that the zinc carboxylate structures we describe are found in each of these reported polymer systems. The present study presents an infrared spectroscopic method to monitor the structural transformations in zinc carboxylates, and it provides detailed insight into the relations between zinc carboxylate structure and properties of the polymer matrix.

It is useful to consider the properties and stability of the different zinc carboxylate types in some more detail. The oxo and chain complex can form in a reaction between ZnO and carboxylic acids, producing water in the process:

$$4\,\mathrm{ZnO} + 6\,\mathrm{R{-}COOH} \rightarrow \underset{\text{oxo}}{\mathrm{Zn_4O(R{-}COO)_6}} + 3\,\mathrm{H_2O}$$

$$n\,\mathrm{ZnO} + 2n\,\mathrm{R{-}COOH} \rightarrow \underset{\text{chain}}{\mathrm{[Zn(R{-}COO)_2]_n}} + n\,\mathrm{H_2O} \quad (1)$$

where R−COOH can be a pendant carboxylic acid group on a polymer segment or a fatty acid molecule. In many noncrystalline systems, including ionomers and molten zinc soaps, the oxo and chain complex can also interconvert according to the following reaction:

https://dx.doi.org/10.1021/acsapm.0c00979
ACS Appl. Polym. Mater. 2020, 2, 5674−5685

$$\underset{\text{oxo}}{Zn_4O(R{-}COO)_6} + 2\,RCOOH \rightleftharpoons \underset{\text{chain}}{[Zn(R{-}COO)_2]_4} + H_2O \quad (2)$$

In nearly all cases, for instance for commercial zinc ionomers based on poly(ethylene-*co*-methacrylic acid),[14,15] molten zinc soaps,[17] and various zinc carboxylates in solution,[16] researchers have found that the oxo complex is favored as long as a source of oxygen (usually water) is present to supply the oxygen anion in the oxo complex. Ishioka et al. reported that IR spectral features of the chain complex only appeared in zinc-neutralized ionomers when samples contained an excess of carboxylic acid groups and when they were thoroughly dried to drive off water,[14] pushing the equilibrium in reaction 2 to the right. In contrast, in zinc ionomers based on highly cross-linked polymerized drying oils like oil paint, invariably a mixture of chain and oxo complexes is observed.[1,5,11] While the relative concentration of these two complexes can vary,[17] the chain complex seems to be remarkably stable in oil polymers, even when samples are submerged in water.[23] This surprising observation leads us to hypothesize that perhaps the strongly cross-linked nature of oil polymers constrains movement of the polymer backbone and attached carboxylate groups with the effect of stabilizing the chain complex. A second explanation could be that the polymer network structure or composition induces a large degree of heterogeneity in the local concentrations of water,[24] thereby creating regions with conditions that favor zinc carboxylates in the chain complex geometry. Given this potential difference in the stability and/or local environment for the chain and oxo complex in oil paint ionomers, it is important for our understanding of oil paint degradation to investigate the relative reactivity of the chain and oxo complex toward the formation of zinc soaps. If there is a difference in reactivity between the two complexes, measuring their concentrations could serve as a predictor for the rate of zinc soap-related degradation in oil paint layers.

With regard to the two possible structures for crystalline zinc soaps (Figure 1b), it has been noted that short-chain, dicarboxylic, and unsaturated fatty acids favor the type A geometry, while long-chain saturated fatty acids tend to adopt a type B structure.[18] However, there are signs that also zinc soaps of long-chain saturated fatty acids can crystallize in a metastable type A structure, presumably under conditions where the crystallization process is very fast or where the optimal packing of fatty acids chains is hindered.[25−27] The capacity to quantify the relative concentrations of type A and type B zinc soaps would give insight into the fatty acid composition of crystallized zinc soaps and possibly the local chemical conditions during zinc soap crystallization. This information is very relevant to determine the chemical composition, conservation history, and degradation risks of an oil painting.

In this work, we use oil paint model systems and attenuated total reflection Fourier transform IR (ATR-FTIR) spectroscopy to investigate systematically how pigment concentration, carboxylic acid concentration, and oil viscosity contribute to variations in the relative concentration of chain and oxo zinc carboxylate species in oil paint binding media. Furthermore, we analyze the evolution of these zinc carboxylates during paint drying and during further aging under high humidity conditions that promote oil hydrolysis and ultimately zinc soap formation.

In this research, a major challenge in the analysis of ATR-FTIR spectra is the fact that all four zinc carboxylate types can occur in a single sample at the same time, giving rise to considerable overlap of spectral features (Figure 1a). The bands associated with the crystalline type A and type B structures are relatively constant in shape and relative intensity across samples, which suggests a possibility of modeling spectra as a relatively straightforward linear combination of reference spectra. However, the ν_a COO−Zn bands associated with the oxo and chain complexes in oil paint ionomers are not identical to those of pure reference compounds, and they tend to show variation in width and relative intensity. For example, the high-frequency ν_a COO−Zn band of the chain complex is rather weak or even absent in oil paint systems under some conditions; density functional theory (DFT) calculations suggest this could be due to disorder in the ideal zigzag orientation of the 1D coordination polymer chain.[17] Spectral fitting solves this problem, but with up to nine overlapping bands in a 150 cm^{-1} wavenumber range, the risk of overfitting is ever present. To resolve these issues, we employ a highly constrained band fitting approach that minimizes the numbers of fit parameters and greatly narrows the tolerated ranges of values for fit parameters by incorporating all prior knowledge on the numbers, positions, widths, and relative magnitudes of bands.

The current study marks a great improvement in our understanding of the evolution of zinc carboxylates in aging oil paint, ionomeric polymers, and rubbers. Moreover, we demonstrate the capacity of IR spectroscopy to provide insight into the behavior of metal ions in oil paint and their surrounding molecular environment.

2. EXPERIMENTAL SECTION

2.1. Preparation of Materials. For all experiments, we used the same batches of cold-pressed untreated linseed oil (Kremer Pigmente) and ZnO (nanopowder <100 nm, Sigma-Aldrich). Pigment and oil were mixed using a mortar and pestle in a 1:1 w/w ratio, unless stated otherwise. Paint mixtures were spread on glass slides with a draw-down bar to a wet thickness of 60 μm.

The carboxylate concentration in the paint mixture was varied by mixing increasing amounts of sorbic acid (2,4-hexadienoic acid, Sigma-Aldrich, ≥99%) in the paint mixture from 5% to 20% of the total mass while keeping the pigment/oil ratio constant at 1:1 (w/w).

The binding medium viscosity was varied by replacing up to 100% of the linseed oil in the paint mixture with fatty acid methyl esters of linseed oil (MeLO). Linseed oil was transesterified following the procedure described by Tumosa et al. by stirring overnight with potassium hydroxide and methanol, after which the product could be separated by extraction with dichloromethane.[28] Product purity was confirmed by nuclear magnetic resonance spectroscopy.

The pigment concentration was varied by mixing between 11% and 59% w/w ZnO in linseed oil.

All paint mixtures described above were dried for 7 days in an air-circulated oven at 60 °C (12% RH at 60 °C). For aging of paint mixtures, films were stored in an air-circulated oven up to 45 days at 60 °C either at 12% RH or inside a closed glass container with a saturated solution of NaCl to achieve a RH of 75%.

Zinc palmitate and zinc oleate reference compounds were prepared by precipitations from an aqueous alkaline solution of zinc nitrate and palmitic or oleic acid, as described previously.[17]

2.2. ATR-FTIR Spectroscopy. Infrared spectra of bulk samples were collected on a PerkinElmer Frontier spectrometer equipped with a heatable Pike diamond GladiATR module. Spectra were collected with four scans and 4 cm^{-1} resolution. Unless stated otherwise, spectra were collected on the bottom of paint films after they were lifted from their glass support. For the analysis of the initial paint curing process, freshly prepared paint mixtures were applied directly to the ATR crystal heated to 60 °C and enclosed inside a metal

https://dx.doi.org/10.1021/acsapm.0c00979
ACS Appl. Polym. Mater. 2020, 2, 5674−5685

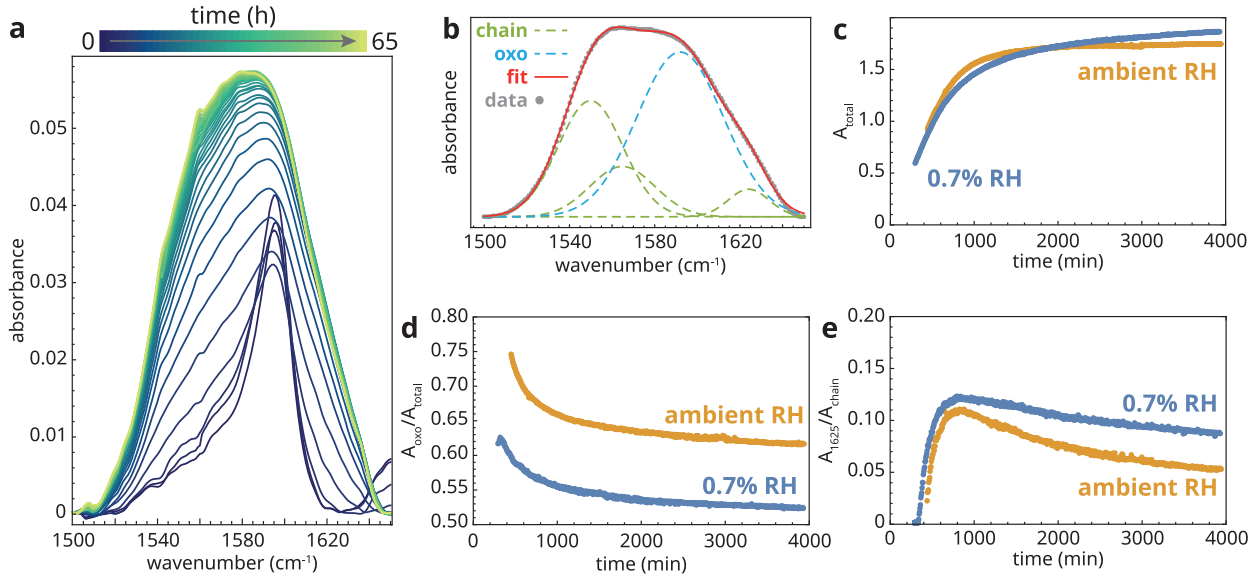

Figure 2. (a) Selection of baseline-corrected ATR-FTIR spectra showing the evolution of the COO−Zn band envelope in a ZnO−LO mixture polymerized at 60 °C under ambient RH conditions. The time between consecutive spectra is 100 min. (b) Example of a constrained fit of the COO−Zn band envelope with four Gaussian band shapes. The dashed curves are the individual Gaussian bands. (c) Total COO−Zn concentration over time. (d) Oxo fraction over time. (e) Chain distortion parameter over time.

cylinder.[7] Spectra were collected every 5 min, while the atmosphere inside the cylinder was flushed with dry air (0.7% RH, 160 ppm water) or was left open to the lab environment (~50% RH).

ATR-FTIR microscopy experiments were performed on a PerkinElmer Spotlight 400 system equipped with a 16-pixel MCT array detector and a germanium crystal ATR sample holder (600 μm diameter footprint). The spectra were averaged over four scans, acquired at 4 cm^{-1} spectral resolution and a pixel step size of 1.56 μm.

2.3. Data Analysis. All fitting of spectroscopic data was performed using custom Wolfram Mathematica scripts. These files, as well as detailed descriptions of the analysis workflow and considerations for constrained band fitting, can be found in the Supporting Information. Briefly, the general procedure for the analysis of each data set (a time series, concentration series, or map of spectra) consisted of a preprocessing step (baseline correction, normalization, and wavenumber range selection), a fit parameter initialization step, and finally a strongly constrained fit on the entire data set to calculate individual band areas. Minor variations of this general approach were applied for different data sets, which is described in the Mathematica notebook files. Aspects of the fitting model that are relevant for the interpretation of the results are discussed in the Results section.

For ATR-FTIR microscopy data, integrated absorbance maps, and regionally averaged spectra were generated by using the ROI Imaging tool of the open-source PyMCA software.[29]

3. RESULTS

The evolution of zinc carboxylate structure in oil paint systems will be discussed in a chronological fashion with respect to oil paint aging. We start with investigating the initial paint drying process (accelerated drying at 60 °C), under both ambient and dry conditions. We will then study model systems with systematic variations in the composition or connectivity of the oil polymer that could influence zinc carboxylate structure. Finally, we investigate the changes in the oil paint under extreme aging conditions (high temperature and humidity), when crystalline zinc soaps are formed.

In the analysis of IR spectral features of ionomeric zinc carboxylates (chain and oxo complex), we will consider three main parameters. (1) Total zinc carboxylate concentration, A_{total}, which is measured as the total ν_a COO−Zn vibration band area. (2) Oxo fraction, A_{oxo}/A_{total}. As a measure of the relative concentrations of oxo and chain complex in zinc ionomers, we define an oxo fraction which is area of the ν_a COO−Zn band corresponding to the oxo complex divided by the total ν_a COO−Zn band area. (3) Chain distortion parameter, A_{1625}/A_{chain}. The relative intensity of the high and low wavenumber ν_a COO−Zn bands of the chain complex are not conserved in zinc ionomers, which may be related to distortion of the ideal chain complex geometry. The fraction of the total chain complex band area that corresponds to the high wavenumber band around 1625 cm^{-1} characterizes this degree of distortion, with lower numbers indicating lower structural order.

3.1. Zinc Carboxylate Evolution during Oil Paint Drying. We studied zinc carboxylate formation in zinc white oil paint (ZnO−LO) during accelerated drying 60 °C under ambient or dry RH conditions. Figure S1 (Supporting Information) shows an example of a set of unprocessed ATR-FTIR spectra collected during paint polymerization.

The evolution of the ν_a COO−Zn band envelope after baseline subtraction in ZnO−LO polymerized under ambient conditions is shown in Figure 2a. Interestingly, when the wet paint mixture was applied to the ATR crystal, a ν_a COO−Zn feature was immediately observed. With a band maximum at 1595 cm^{-1}, this band points to the presence of an oxo complex. This observation indicates that carboxylic acid groups were already present in LO after paint mixing, either due to the typical presence of free fatty acids in unprocessed LO[9] or due to oxidation during paint mixing. There was also some signal at lower wavenumbers (1540−1550 cm^{-1}), possibly weak absorption from chain complex zinc carboxylates.

To analyze the changes in zinc carboxylate structure and concentration during drying, we constructed a fitting model based on four Gaussian bands: one band centered close to 1590 cm^{-1} for the oxo complex and three bands centered around 1550, 1565, and 1625 cm^{-1} for the chain complex. Figure 2b shows an example of such a fit. In these fits, band positions and widths were fixed, while the relative intensity of

https://dx.doi.org/10.1021/acsapm.0c00979
ACS Appl. Polym. Mater. 2020, 2, 5674−5685

two lowest wavenumber bands was constrained, yielding a total of four fit parameters. To obtain meaningful results, we wished to use a single model for each experiment run. However, while the R^2 values of the fit converged to values very close to 1 at curing times >400 min, the earliest stages of curing were not adequately described by the constrained fitting model with fixed band widths and band positions (see Figure S2). Rather than allowing more variation in fit parameters, we chose to omit the early stages of curing from our analysis and consider only fit results with $R^2 > 0.99$. As described in the Supporting Information, the values for the fixed band width and position parameters were determined by performing a fit on the spectral average of each data series to ensure reproducible results. Nevertheless, band widths never varied more than 5% between data series and band positions never shifted by more than 2 cm^{-1}.

As expected, the total ν_a COO−Zn band area increased during oil paint curing (Figure 2c). The concentration of zinc carboxylates reached a plateau around 2000 min under ambient RH conditions, while under 0.7% RH the zinc carboxylates kept forming slowly even after 4000 min of curing. During oil polymerization, most carboxylic acid groups are formed on the unsaturated alkyl chains in the triglyceride monomers through a sequence of bis-allylic hydrogen abstraction, the formation of radical oxide groups, a β-scission reaction, and subsequent oxidation.[2,4] These carboxylic acids are likely to react quickly with ZnO to form zinc carboxylates and water (reaction 1). Given this relation between *cis* C═C bonds and zinc carboxylates in the oil matrix, we compared the consumption of *cis* C═C bonds and the formation of zinc carboxylates, shown in Figure S2. There was a very strong anticorrelation between the intensity of the *cis* C═C−H stretch vibration band at 3010 cm^{-1} and the bands corresponding to the oxo and chain complex. This anticorrelation is the result of two effects: (1) because *cis* C═C bond consumption stands at the start of the reaction pathway leading to zinc carboxylates, COO−Zn formation will slow down as the double bond concentration decreases; (2) the consumption of double bonds leads to an increasing degree of polymerization, and this increased viscosity of the reaction mixture decreases all reaction rates, including the rate of COO−Zn formation.

Interestingly, the chain and oxo complex do not form at the same rate. Figure S2 shows that the oxo complex forms faster initially, while at long time scales most of the zinc carboxylates are forming as chain complexes, especially at ambient humidity. This conclusion is also evident when considering the time profiles of the oxo fraction in Figure 2d. During oil polymerization the oxo fraction decreases, indicating that the chain complex is more likely to form at longer time scales. There is also a clear effect of humidity on the oxo fraction. At low humidity, the oxo complex only accounts for approximately half of the total ν_a COO−Zn band area in the polymerized paint film, while the oxo fraction is close to 0.62 under ambient RH conditions. This observation suggests the formation rate of the oxo complex is at least partially determined by the concentration of water inside the paint film during oil polymerization, which is affected by the release of water through ZnO breakdown (reaction 1) and water absorption from the environment.

We can investigate the role of water further by considering the O−H stretch vibration bands in the region 3100−3600 cm^{-1}, which are largely caused by water molecules inside the polymer matrix (see Figure S2). Because of overlap with the O−H stretch vibration band of alcohol groups that may form during oil polymerization, it is challenging to calculate reliable water concentrations on the basis of the current set of spectra. However, it has been reported that the concentration of alcohol groups does not depend strongly on humidity in this initial polymerization process.[30] Assuming a similar alcohol concentration for ambient and low RH conditions, Figure S2e shows that the water concentration is considerably higher at ambient RH than under dry conditions, which explains why the oxo fraction values are consistently higher at ambient RH (Figure 2d). Because there is little change in water concentration after 600 min of polymerization, water does not explain the downward trend in oxo fraction with time. We propose instead that with increasing carboxylate concentrations on longer time scales the chain complex becomes more stoichiometrically favored over the oxo complex, which has a higher Zn:COO ratio (reaction 2).

Regardless of the interpretation of the trends in the oxo fraction, two important observations are worth pointing out. First, the chain complex also forms under ambient humidity conditions even though it is thought to be less stable than the oxo complex in the presence of water. This result suggests that there are regions inside the curing paint with low water content and/or high carboxylic acid concentration that promote the formation of chain complex. Second, the oxo complex also forms under very low humidity conditions, which demonstrates that there is a substantial amount of water present or generated inside the polymerizing paint film regardless of environmental conditions. Taking these two observations together, we can conclude that there is considerable heterogeneity in these oil paint films, with varying local conditions that favor either chain or oxo complex formation. This conclusion is in line with recent work by Di Tullio and co-workers, who used nuclear magnetic resonance spectroscopy to demonstrate that the diffusion of water is restricted in oil paint films and that several regions exist with different water concentrations and mobilities.[24]

Considering the changing structure of the chain complex during paint drying, we consistently observed a maximum in the chain distortion parameter after ∼750 min (Figure 2e). In the reference chain complex spectrum in Figure 1b of pure liquid zinc palmitate, the value of A_{1625}/A_{chain} is 0.28. In contrast, in curing ZnO−LO paint the value never reached higher than ∼0.12, which suggests that the structure of the chain complex in oil paint is always disordered to some extent. The presence of a maximum in A_{1625}/A_{chain} could indicate that optimizing the geometry of the chain complex in oil polymers takes time (leading to an increase in the chain distortion parameter at short time scales), while at long time scales the increasingly polymerized oil medium prevents optimization of the chain complex geometry (leading to a decreasing trend in A_{1625}/A_{chain}). It is interesting to note that there is also a relation between humidity and the chain distortion parameter. Under ambient RH conditions, the absolute area of the 1625 cm^{-1} band actually decreased at long time scales, while it remained approximately constant under a dry atmosphere. This humidity effect could point to differences in polymer network structure or plasticity that affect the range of motion of polymer segments during chain complex formation.

It is evident that there is a potential abundance of useful information about polymer structure and reactivity in these ATR-FTIR spectra of drying ZnO−LO paint. However,

https://dx.doi.org/10.1021/acsapm.0c00979
ACS Appl. Polym. Mater. 2020, 2, 5674−5685

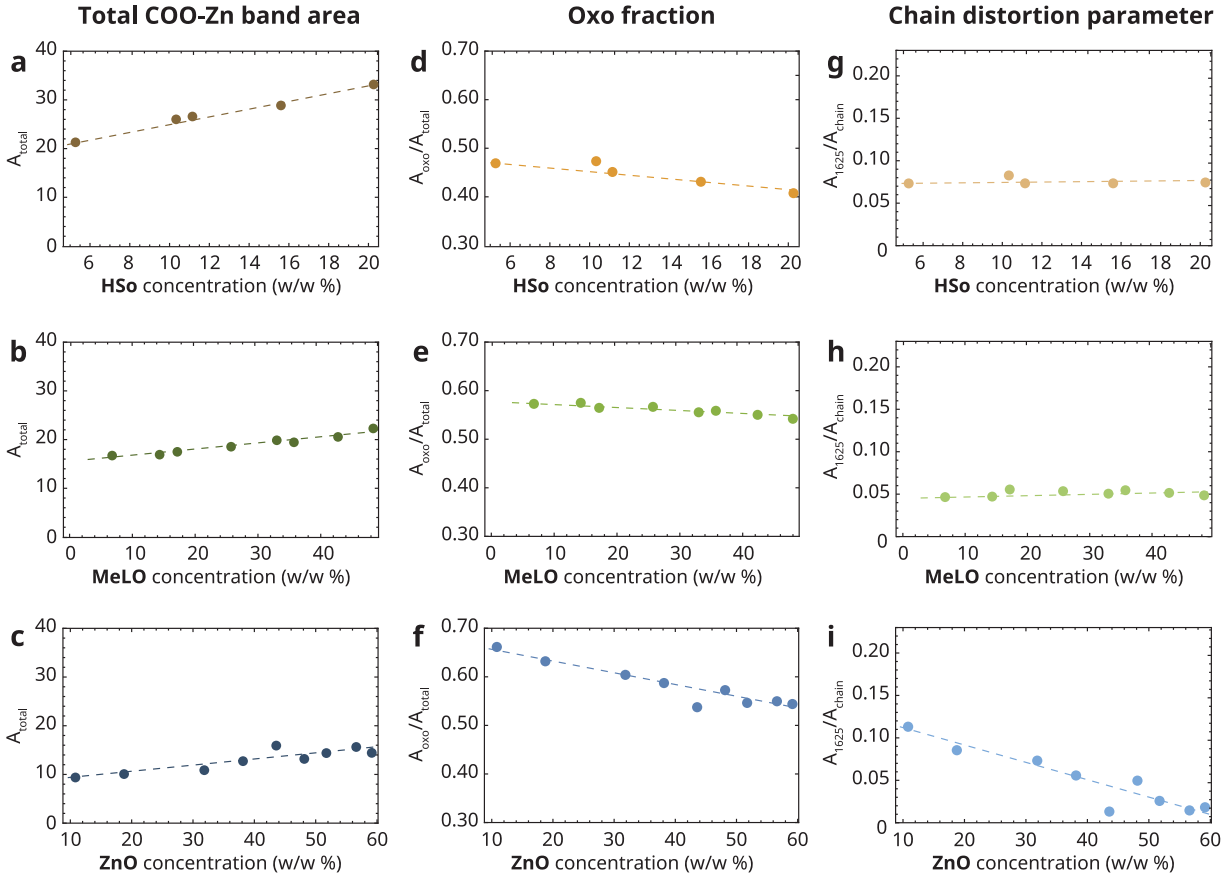

Figure 3. (a–c) Total COO–Zn concentrations, (d–f) oxo fractions, and (g–i) chain distortion parameters for ZnO–LO paint films in which the concentration of (a, d, g) sorbic acid (HSo), (b, e, h) linseed oil methyl esters (MeLO), or (c, f, i) zinc oxide was varied. In the HSo and MeLO series, the ZnO:LO ratio was kept constant at 1:1 (w/w). Prior to band fitting, all spectra were normalized to the CH_2 bend vibration band at 1455 cm^{-1} and baseline-corrected. Concentrations are expressed as w/w % of the total paint mixture. All dashed lines are guides to the eye.

reliably interpreting the spectral features or the effects of humidity is challenging in these complex systems. With the aim of supporting interpretations, we have systematically modified the cured ZnO–LO paint system to study the effect of carboxylic acid concentration, paint viscosity, and pigment content.

3.2. Variations in Cured ZnO–LO Film Composition. We will discuss the effects of three types of modifications to the ZnO–LO paint system. The carboxylic acid concentration was varied by mixing increasing amounts of 1,3-hexadienoic acid (sorbic acid, HSo) together with ZnO and LO (1:1 w/w), which copolymerize with the unsaturated fatty acid chains in LO during paint drying. The initial viscosity of the paint mixture was decreased by replacing increasing portions of the LO in the paint mixture with fatty acid methyl esters (LO transesterified with methanol, MeLO), thereby reducing the number of glycerol linkers between fatty acid chains. Finally, the ZnO concentration was varied from 10% to 60% w/w. All modified paint films were dried at 60 °C (12% RH) for 1 week.

3.2.1. Total COO–Zn Concentration. As was found in earlier research, the total COO–Zn concentration increased linearly with the addition of HSo (Figure 3a).[4] This trend supports previous conclusions that given an excess ZnO content (usually the case in a typical oil paint), the concentration of zinc carboxylate species is governed by the availability of carboxylic acid groups. More surprising is the result that the COO–Zn concentration increased with MeLO content, rising to a concentration equivalent to a 6% HSo concentration for a paint mixture where all LO was replaced by MeLO (Figure 3b). The most likely explanation for this trend lies in the relation between reaction kinetics in the polymer and the degree of polymerization. With higher MeLO concentration, it takes longer for the drying ZnO paint mixture to increase in viscosity and cure to a solid film, which results in a longer time window with relatively fast reaction kinetics for the formation of carboxylic acid groups.

The rising trend in zinc carboxylate concentration with increasing ZnO content, shown in Figure 3c, is less well-understood. While rising concentrations of zinc carboxylates with increasing ZnO content seem intuitive, it is important to note that the total concentration of zinc ions in the system is higher than the carboxylic acid concentration throughout the sample series. Casting further doubt on a stoichiometric explanation for the increasing trend COO–Zn concentration, we did not find any sign in the ATR-FTIR spectra of an increasing concentration of free COOH groups at lower pigment content, which suggests that it is really the overall concentration of carboxylic groups that changes in this sample series. Zinc ions are occasionally used as auxiliary driers in alkyd coating formulations. According to some sources, zinc ions slow down autoxidation and delay surface skin formation, leading to a more homogeneously dried, harder, and more glossy polymer film.[31] However, Sturdy and co-workers recently reported quartz-crystal microbalance measurements that showed an increased alkyd autoxidation rate with increasing ZnO pigment content, with a doubling of the

https://dx.doi.org/10.1021/acsapm.0c00979
ACS Appl. Polym. Mater. 2020, 2, 5674–5685

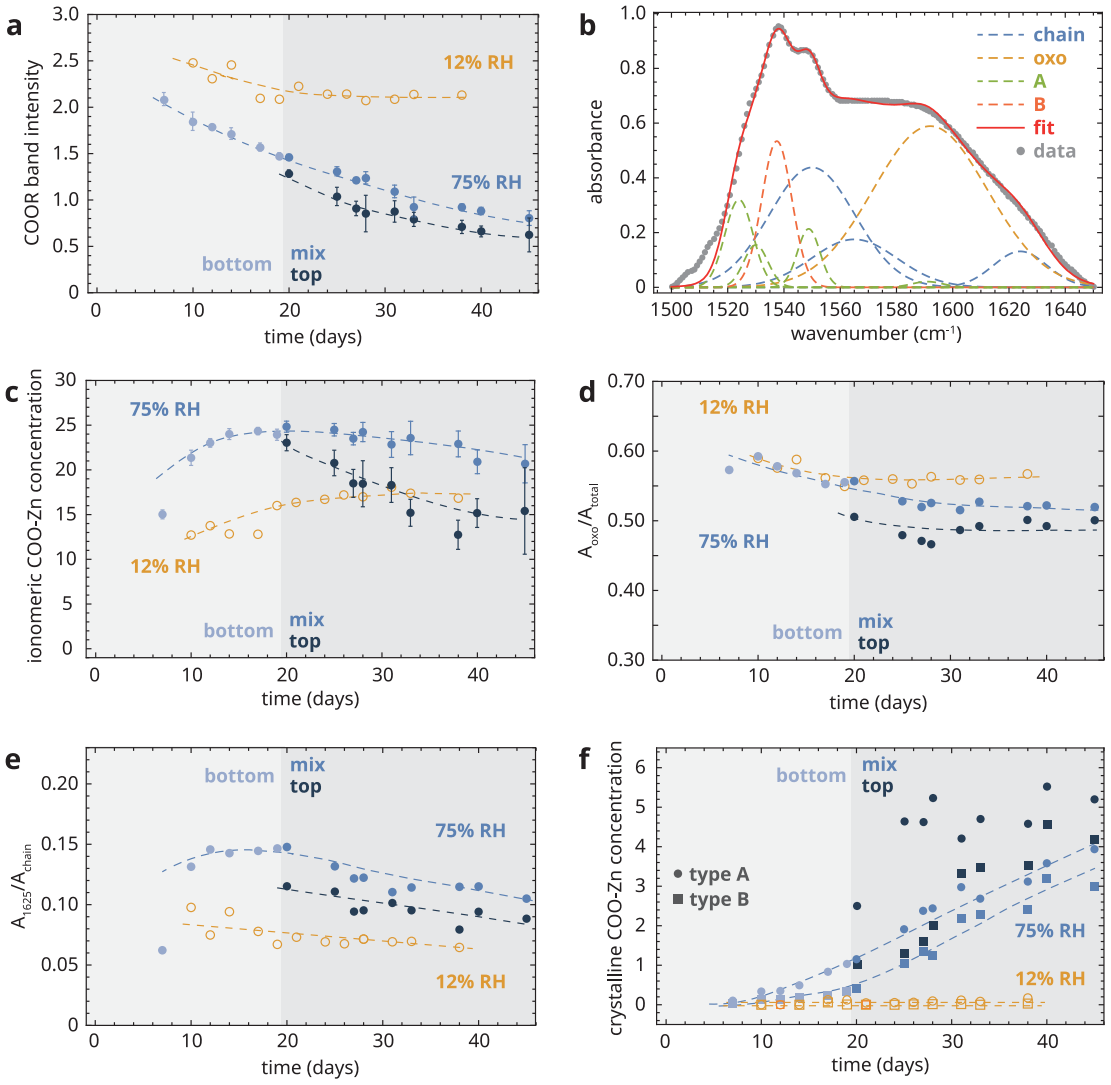

Figure 4. (a) Evolution of ester band height (absorbance at 1738 cm^{-1}) during aging. (b) Example of a strongly constrained fit of the ν_a COO−Zn band envelope using nine Gaussian band shapes. (c) Total ionomeric zinc carboxylates concentration over time. (d) Evolution of the oxo fraction during aging. (e) Chain distortion parameter as a function of aging. (f) Increasing concentration of type A and type B zinc soaps during aging. All aging was performed at 60 °C. Prior to band fitting, all spectra were normalized to the CH_2 bend vibration band at 1455 cm^{-1} and baseline-corrected. Error bars represent one standard deviation based on five replicate measurements on different areas of the sample. Bottom, top, and mix refer to measurements take on either the surface of the film in contact with the glass support, the top surface exposed to the environment, or on powdered paint samples, respectively. All dashed lines are guides to the eye.

oxidation rate in a 50% w/w ZnO−binder mixture compared to the empty alkyd binder.[32] While a mechanism for this accelerating effect was not reported, the rising trend in COO−Zn concentration with ZnO content in Figure 3c is in agreement with the notion that ZnO enhances the autoxidation rate of drying oil.

3.2.2. Oxo Fraction. The oxo fraction showed a decreasing dependence on the concentration of added HSo (Figure 3d). The lower values for the oxo fraction at high carboxylate content are due to the difference in stoichiometry in the oxo and chain complex, causing a small shift in the equilibrium between the oxo and chain complex toward the latter under high acid conditions. The oxo fraction was weakly dependent on the MeLO content in this oil paint model system (Figure 3e). The weakness of this trend suggests that the viscosity of the initial paint mixture is not a factor that strongly influences the relative concentration of chain and oxo complexes. We did observe a large effect of ZnO content on the oxo fraction, as shown in Figure 3f. The downward trend is most likely linked to the concentration of carboxylate groups in the polymer. Indeed, comparing the oxo fractions with the values for A_{total} in Figure 3a−c, the highest oxo fractions are consistently found for the lowest total COO−Zn concentrations. This relation is clearly illustrated by the correlation plot of A_{total} and A_{oxo}/A_{total}, shown in Figure S3. Given this link between oxo fraction and total carboxylate concentration, we can attribute the decreasing oxo fraction that was observed in Figure 2d during paint drying to a rising carboxylate concentration.

3.2.3. Chain Distortion Parameter. The chain distortion parameter showed no dependence on the HSo concentration (Figure 3g). There was also no clear variation observed in the chain distortion parameter with increasing MeLO content (Figure 3h), which suggests that the addition of MeLO does not strongly influence rigidity of the polymer once it is fully cured. This observation is somewhat surprising given the lack of glycerol linkers between the fatty acid chains in MeLO and

https://dx.doi.org/10.1021/acsapm.0c00979
ACS Appl. Polym. Mater. 2020, 2, 5674−5685

the decreasing trend in A_{1625}/A_{chain} with curing (Figure 2) and aging (discussed in section 3.3.2). Possibly, the lower viscosity of MeLO increases the polymerization rate to such an extent that the faster formation of cross-links balances the absence of glycerol linkers.

ZnO content was the only variable that had a strong effect on A_{1625}/A_{chain}, which decreased with higher pigmentation (Figure 3i). Sturdy and colleagues reported an increase in T_g and a broader relaxation time distribution with increasing ZnO pigment content in alkyd binders, which they attributed to slower polymer dynamics in the vicinity of pigment particles.[32] These effects of ZnO, leading to an overall stiffer polymer network, would be an explanation for the decrease in structural order in the chain complex with higher ZnO content.

3.3. Zinc Carboxylate Evolution during Aging. The experiments described so far give important clues about the factors that can influence the concentration of zinc carboxylates in ZnO−LO mixtures and the relative concentrations of oxo and chain complexes. The situation becomes more complex when oil paint films age for long periods of time. When the aging conditions promote the hydrolysis of ester bonds in the polymerized oil network, a concentration of free saturated fatty acids can build up that reacts with oxo and chain complexes to form crystalline zinc soaps.

3.3.1. Polymer Breakdown during Aging. We performed a paint aging experiment where ZnO−LO paint films were dried and aged at 60 °C at either 12% RH or 75% RH. Figure S4 shows a series of normalized ATR-FTIR spectra collected during aging under high humidity. These spectra show a clear decrease in the intensity of C−O vibrations and other bands associated with the polymerized oil network in the region 1000−1300 cm^{-1} as well as a decreasing ester carbonyl band at 1738 cm^{-1}. These changes all indicate breakdown of the polymer network during aging. At the same time, there are significant changes in the ν_a COO−Zn band envelope with the appearance of sharp bands of crystalline zinc soaps of both type A and type B.

Figure 4a shows the steady decrease of the ester band at 1738 cm^{-1} over the course of 45 days of aging at 75% RH, while at 12% RH the band remained mostly constant. This decrease is the result of water-induced hydrolysis reactions, which means that the concentration of carboxylic acid or carboxylate groups strongly increased during aging. The degradation of the polymer network was also experienced during sample handling. While we intended to measure all spectra at the bottom of the films as those would be more representative of the film as a whole, after 19 days the films aged at high humidity were too brittle to be lifted off the glass support. Therefore, after 19 days all films were measured both on the top of the films and on powdered samples (denoted "mix" in the Figure 4). In all subsequent analyses, the spectra collected on the top of the films represented a level of aging that was more progressed than spectra collected on powdered samples. Finally, because the data showed increasingly large variation between measurements on identically prepared samples with increasing exposure to humid aging conditions, all spectra on samples aged at 75% RH were collected in 5-fold and averaged.

3.3.2. Noncrystalline Zinc Carboxylate Structures. With the appearance of crystalline zinc soap bands, fitting the ν_a COO−Zn band envelope accurately became more challenging. There is extensive overlap of bands especially in the range 1500−1560 cm^{-1}, making unconstrained fitting impossible. We chose to model the type B COO−Zn band with a single Gaussian band shape, while type A zinc soaps were modeled with four Gaussians. In both cases, initial estimates of the widths and center frequencies were obtained by carrying out a fit on the spectra of the pure model structures shown in Figure 1, after which the relative intensities of the bands of type A zinc soaps were fixed. During the fit of the entire spectral series, the widths and positions of the chain and oxo complex bands were the same as those in Figure 2b. For the crystalline zinc soaps, the band positions were allowed to vary 4 cm^{-1} around the center frequency of the model structures, while the widths were allowed to vary by 10%. Figure 4b shows an example of a spectral fit with these constrained width and position parameters and five unconstrained intensity parameters. The fitting algorithm converged for all spectra and, apart from the small band tail at 1500−1515 cm^{-1}, gave an excellent match between model and data.

The total concentration of ionomeric zinc carboxylates increased initially during aging (Figure 4c). At high humidity, the total zinc carboxylate concentration was much higher than at low humidity, reaching a maximum after ∼20 days. This result demonstrates that carboxylic acid groups keep steadily forming during paint aging, that ZnO is consumed in this process, and that humidity strongly increases the zinc carboxylate concentration by promoting ester hydrolysis in the oil polymer network. After 20 days at 75% RH, the zinc carboxylate concentration started declining, indicating that the rate of the zinc soap crystallization process that consumes ionomeric zinc carboxylates was higher than ester hydrolysis beyond this time. This decrease was especially evident at the top of the paint film.

The oxo fraction was initially very similar for the paint films aged at dry and humid conditions, as shown in Figure 4d. Given that there was a large difference in zinc carboxylate concentration between the dry and humid films, this similarity in oxo fractions seems to contradict the link between A_{total} and the oxo fraction illustrated in Figure 3 and Figure S3. Clearly, the oxo fraction is not solely determined by the total carboxylate concentration, but it is also dependent on the water concentration inside the paint films. With the onset of zinc soap formation, the oxo fraction decreased to values below those of the film aged at 12% RH. The effect was again more pronounced at the top of the paint film. As is shown in Figure 3, the decreasing oxo fraction is likely to be the result of the increasing concentration of carboxylate groups, which favors the formation of chain complex zinc carboxylates. Additionally, there could be differences in reactivity toward zinc soap formation between oxo and chain complexes. Because these complexes are both formed and consumed during oil paint aging, the individual formation and consumption rates cannot be studied with this data. However, the data recorded on the top of the paint layers, where there was net consumption of ionomeric zinc carboxylates with an approximately constant oxo fraction, do suggest that the difference in reaction rate between oxo and chain complexes is not large.

The chain distortion parameter decreased slowly with time regardless of humidity (Figure 4e). This decrease probably reflects the increase in oil polymer network stiffness due to the evaporation of low molecular weight polymer fragments as the paint continues aging. Interestingly, A_{1625}/A_{chain} was consistently higher for the paint film aged at 75% RH. Upon comparison of these differences with Figure 4a, the concentration of remaining ester groups is considerably

https://dx.doi.org/10.1021/acsapm.0c00979
ACS Appl. Polym. Mater. 2020, 2, 5674−5685

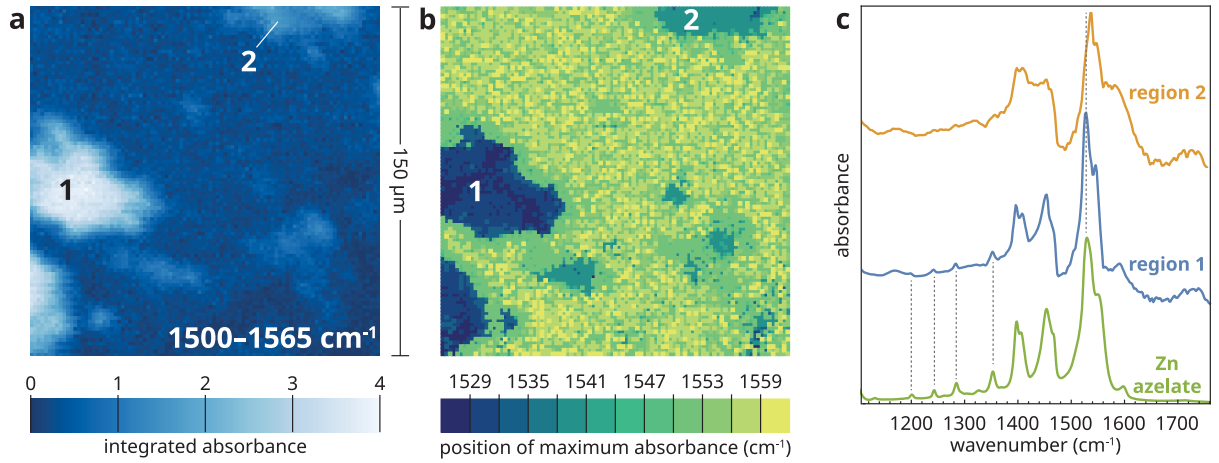

Figure 5. (a) Integrated absorbance map (1500−1565 cm^{-1}, with a baseline between the edges of the integration range) of the top surface of a ZnO−LO film aged at 75% RH and 60 °C for 38 days. (b) Band maximum map of the same spatial region showing the position of maximum absorbance in the range 1526−1562 cm^{-1}, which allows easy distinction between dominant zinc carboxylate species. (c) Comparison between extracted averaged spectra in regions 1 and 2 in (a, b) and a reference spectrum of zinc azelate.

lower in the paint films aged at high humidity, which could reduce polymer network rigidity. Additionally, while the paint samples were removed from the humidity chamber for measurements, polymer stiffness in the 75% RH samples could be affected by the presence of relatively high water concentrations inside the paint films.

3.3.3. Crystalline Zinc Soap Structures. It is interesting to consider the structure of the crystalline zinc soaps that formed in ZnO−LO during aging. Figure 4f shows that after 38 days of aging at 60 °C and 12% RH the concentration of zinc soaps was still negligible. At 75% RH, zinc soaps were detected after ∼10 days, and their concentration kept rising steadily. Especially in the measurements at the top of the paint films, there were very large fluctuations in the intensity of the ν_a COO−Zn bands of the crystalline zinc soaps between IR spectra collected on identically prepared samples, leading to large degrees of scatter. However, the concentration of zinc soaps was consistently higher at the top surface than in the powdered paint films.

The band fitting approach illustrated in Figure 4b allows distinction between zinc soaps with a type A or type B structure (see Figure 1). The type A zinc soaps were first to be detected, and their spectral features remained more intense than those of type B zinc soaps. The type B spectral features can be uniquely associated with crystalline zinc soap complexes of long-chain saturated fatty acids like stearate and palmitate.[18] The identity of the type A zinc soaps is more difficult to establish because both short-chain and long-chain fatty acid zinc soaps can crystallize in this geometry.[18] There is information about the length of crystallized fatty acid chains in the series of progression bands caused by coupled CH_2 vibrations in the region 1180−1380 cm^{-1}.[33] In the bulk ATR-FTIR spectra that have been considered so far, however, the concentration of zinc soaps is low compared to the overlapping spectral features caused by the polymer network, which makes accurate detection of these weak progression bands challenging.

3.3.4. ATR-FTIR Microscopy of Aged ZnO−LO. To further investigate the composition of the type A zinc soaps, we measured ZnO−LO films aged under humid conditions with ATR-FTIR microscopy. Figure 5a shows a map of integrated absorbance of the ν_a COO−Zn bands of crystalline zinc soaps. Multiple microscopy measurements on randomly selected areas on the surface of the sample showed very large variations in the number and size of areas rich in zinc soaps. This heterogeneity on a millimeter length scale is in agreement with the large amount of scatter observed in the zinc soap band intensity at the top surface shown in Figure 4f. Within the 150 × 150 μm window of Figure 5a, there were several regions with a high concentration of crystalline zinc soaps. The band position map in Figure 5b shows the position of maximum absorbance in the region 1526−1562 cm^{-1}, which allows for an easy idenfication of the dominant zinc carboxylate species across the map. Here, a blue color corresponds to type A zinc soaps, green corresponds to type B zinc soaps, and the yellowish background signal indicates that ionomeric zinc carboxylates are dominant. In this map, regions rich in type A (region 1) and type B (region 2) zinc soaps can be distinguished. The extracted spectra in Figure 5c show that the two regions indeed exhibit different positions of the ν_a COO−Zn band maximum, lying at 1536 cm^{-1} in region 2 and at 1527 cm^{-1} in region 1. The concentration of type A zinc soaps in region 1 is high enough for its corresponding spectrum to show a clear set of four CH_2 progression bands. Their positions match those of a zinc azelate (zinc nonanedioate) reference spectrum, confirming previous findings of high concentrations of zinc azelate in model and historical zinc white paint films that were strongly oxidized and hydrolyzed.[18,34] Unfortunately, because of the lower purity of the type B zinc soaps in region 2, it was not possible to detect a clear set of CH_2 progression bands and identify the fatty acid composition of these zinc soaps.

Finally, the ATR-FTIR microscopy data allow a more detailed investigation of the consumption of oxo and chain complex zinc carboxylates during zinc soap crystallization. We performed a fit of the ν_a COO−Zn band envelope for each of the spectra in the sample area shown in Figure 5. While these fits on microscopy data were less accurate than those on bulk ATR-FTIR spectra because of higher noise levels and residual water vapor contributions, analysis of the spatial distribution of the zinc carboxylates does suggest a difference in reaction rates between the oxo and chain complexes. Figure S5a,b demonstrates clearly that the ionomeric zinc carboxylates have been almost completely consumed in regions of the

https://dx.doi.org/10.1021/acsapm.0c00979
ACS Appl. Polym. Mater. 2020, 2, 5674−5685

sample with a high concentration of crystalline zinc soaps. If both types of ionomeric zinc carboxylate would react with equal rates to form crystalline zinc soaps, one would expect a constant ratio between the band areas of the oxo and chain species for any pixel in the data set. Figure S5c shows the correlation between normalized total band areas for the oxo and chain complex, where a collection of off-diagonal pixels can be observed with a relative oxo complex concentration that deviates from the majority of the pixels. The region in the map corresponding to these pixels can be visualized by plotting a map of $A_{oxo} - A_{chain}$, as shown in Figure S5d. While there is some background noise, the regions corresponding to a high crystalline zinc soap concentration clearly stand out. On the basis of this result, we propose the hypothesis that while local concentrations of both oxo and chain complex are ultimately consumed during zinc soap formation, the oxo complex is more stable than the chain complex under typical conditions in aging ZnO−LO paint, causing a slower oxo consumption rate.

4. DISCUSSION

The experiments discussed above are a good illustration of the complexity of oil paint chemistry. While model systems are essential to develop an understanding of the relation between molecular structure or composition and paint degradation, it is clearly not straightforward to systematically vary single parameters and study their effect. For example, the addition of carboxylic acids like sorbic acid to an oil paint mixture does not necessarily lead to a high proton concentration in the polymerized paint film. In the case of ZnO−LO paint, we have demonstrated that most carboxylic acid groups quickly react with the pigment, leading to high concentrations of zinc carboxylates and water instead. Moreover, it remains challenging to separate the direct effects of functional group concentrations from their indirect kinetic effects. For example, reduction of the number of glycerol linkers by replacing LO with MeLO intuitively causes a reduced polymer network connectivity, but this MeLO replacement will also undoubtedly affect the rate of cross-linking reactions, making it very difficult to predict the properties of the final polymerized network.

While the experiments described here mostly concern the formation of zinc carboxylates, two broader conclusions that are generally relevant for chemistry in oil paintings and other complex polymer systems are worth highlighting. First, despite the slow reaction kinetics in highly cross-linked oil polymer networks, the average chemical composition of a paint is still mostly governed by the relevant chemical equilibria. In the case of zinc carboxylates, reaction 2 has proven to be very powerful to predict the effects of increasing concentrations of carboxylic acid or water. For other chemical transformations related to oil paint degradation, elucidating the relevant reactions should have high priority. Second, the presence of both oxo and chain complexes in ZnO−LO paints demonstrates that different local chemical environments can coexist even within a single paint layer with a relatively simple composition. This heterogeneity in local conditions can be an important factor to consider when trying to explain the many different products of reactions involving pigments or the oil polymer that are commonly observed in oil paints.

Prior to the experiments described in this study, the interpretation of the parameter A_{1625}/A_{chain} as a measure for disorder was based mostly on the comparison of density functional theory calculations of chain complex segments in the zigzag conformation of crystalline zinc crotonate and a theoretical stretched-chain conformation.[17] With the exception of the anomalous effect of MeLO concentration in Figure 3h, all presented data are in line with the hypothesis that A_{1625}/A_{chain} is related to polymer network rigidity because the parameter decreased during initial polymerization, during long-term aging, and with increasing ZnO content.

In this work, evidence has been presented that suggests a difference in reactivity of the chain and oxo complex toward zinc soap formation. The study of this effect is complicated by the fact that during oil paint aging the overall chain complex concentration can increase due to a hydrolysis-driven increasing carboxylate concentration, while locally the chain complex concentration can decrease faster than the oxo complex near regions rich in crystalline zinc soaps. These two effects can lead to an apparent contradiction between bulk and microscopy FTIR spectroscopic data. To study these processes in more detail, measurements are needed where the same sample area is monitored over time during the formation of zinc soaps. Such experiments are currently being developed.

Finally, the study of molecular structure in zinc white oil paints can be developed further by the application of computational modeling. Now that the individual zinc carboxylate structures and the relevant reaction pathways have been resolved, it has become possible to simulate the evolution of zinc carboxylates both over time and, with assumptions about the diffusion of reactive species, in space. Such simulations would serve to support interpretations of complex experimental results and allow the study of the influence of parameters that are difficult control experimentally.

5. CONCLUSIONS

With the recent elucidation of the structures of zinc carboxylates in zinc white oil paints, we have demonstrated a method to monitor the evolution of zinc carboxylate structure through detailed analysis of ATR-FTIR spectra collected during paint drying and aging. Here, it was found that the total concentration of ionomeric zinc carboxylates (oxo and chain complex) increases with time, but also with increasing ZnO pigment content, at high humidity, and with lower viscosity of the initial paint mixture. The fraction of the ionomeric zinc carboxylates that adopt an oxo complex structure depends mostly on the total carboxylate concentration in the paint film, with higher carboxylate concentrations leading to lower oxo fractions. Additionally, there is a positive correlation between environmental humidity and the oxo fraction. Finally, we have found evidence that the structure of the chain complex is affected by the stiffness of the surrounding polymer, becoming increasingly disordered with time and with higher ZnO content. With these results, it has become easier to assess the past or current internal chemical conditions inside aging oil paints, and we have shed light on the complex behavior of metal ions in ionomer systems.

For the conservation of the many important artworks that contain zinc white pigments, this research provides the foundation to start searching for metrics that can be obtained from routine FTIR spectroscopy measurements on paint samples to estimate the risks of future degradation. Moreover, to actively influence the rate of paint degradation, it has become clear once again that a better control of the concentration of water inside paint films has the potential to prolong the lifetime of paintings. Future research should be directed at quantifying the relations between environmental

https://dx.doi.org/10.1021/acsapm.0c00979
ACS Appl. Polym. Mater. 2020, 2, 5674−5685

humidity, local water concentration inside paint layers, and polymer network breakdown as well as finding feasible methods to control water concentrations in real artworks.

■ ASSOCIATED CONTENT

Supporting Information

The Supporting Information is available free of charge at https://pubs.acs.org/doi/10.1021/acsapm.0c00979.

Details on data analysis and additional figures (PDF)

Mathematica notebook files (ZIP)

■ AUTHOR INFORMATION

Corresponding Author

Joen Hermans − *Van 't Hoff Institute for Molecular Sciences, University of Amsterdam, 1090GD Amsterdam, The Netherlands; Conservation & Science, Rijksmuseum, 1070DN Amsterdam, The Netherlands;* orcid.org/0000-0002-9446-9904; Email: j.j.hermans@uva.nl

Authors

Marit Beerse − *Van 't Hoff Institute for Molecular Sciences, University of Amsterdam, 1090GD Amsterdam, The Netherlands*

Katrien Keune − *Van 't Hoff Institute for Molecular Sciences, University of Amsterdam, 1090GD Amsterdam, The Netherlands; Conservation & Science, Rijksmuseum, 1070DN Amsterdam, The Netherlands*

Piet Iedema − *Van 't Hoff Institute for Molecular Sciences, University of Amsterdam, 1090GD Amsterdam, The Netherlands*

Sander Woutersen − *Van 't Hoff Institute for Molecular Sciences, University of Amsterdam, 1090GD Amsterdam, The Netherlands;* orcid.org/0000-0003-4661-7738

Complete contact information is available at: https://pubs.acs.org/10.1021/acsapm.0c00979

Author Contributions

M.B. performed experiments and initial analysis. K.K., P.I., and S.W. contributed to discussions and edited the manuscript. J.H. conceived and supervised the project, performed experiments, analyzed the data, and wrote the manuscript.

Notes

The authors declare no competing financial interest.

■ ACKNOWLEDGMENTS

J.H. received funding from the Bennink Foundation/ Rijksmuseum Fonds and The Netherlands Organization for Scientific Research (NWO) under project number 016.Veni.192.052. K.K. and J.H. received funding for equipment from Fonds1999.

■ REFERENCES

(1) Osmond, G.; Boon, J. J.; Puskar, L.; Drennan, J. Metal stearate disributions in modern artists' oil paints: surface and cross-sectional investigation of reference paint films using conventional and synchrotron infrared microspectroscopy. *Appl. Spectrosc.* **2012**, *66*, 1136−1144.

(2) van Gorkum, R.; Bouwman, E. The oxidative drying of alkyd paint catalysed by metal complexes. *Coord. Chem. Rev.* **2005**, *249*, 1709−1728.

(3) De Viguerie, L.; Payard, P. A.; Portero, E.; Walter, P.; Cotte, M. The drying of linseed oil investigated by Fourier transform infrared spectroscopy: Historical recipes and influence of lead compounds. *Prog. Org. Coat.* **2016**, *93*, 46−60.

(4) Baij, L.; Chassouant, L.; Hermans, J. J.; Keune, K.; Iedema, P. D. The concentration and origins or carboxylic acid groups in oil paint. *RSC Adv.* **2019**, *9*, 35559−35564.

(5) Hermans, J. J.; Keune, K.; van Loon, A.; Iedema, P. D. An infrared spectroscopic study of the nature of zinc carboxylates in oil paintings. *J. Anal. At. Spectrom.* **2015**, *30*, 1600−1608.

(6) Hermans, J.; Keune, K.; Van Loon, A.; Corkery, R. W.; Iedema, P. Ionomer-like structure in mature oil paint binding media. *RSC Adv.* **2016**, *6*, 93363−93369.

(7) Baij, L.; Hermans, J. J.; Keune, K.; Iedema, P. Time-Dependent ATR-FTIR Spectroscopic Studies on Fatty Acid Diffusion and the Formation of Metal Soaps in Oil Paint Model Systems. *Angew. Chem., Int. Ed.* **2018**, *57*, 7351−7354.

(8) Hermans, J.; Osmond, G.; van Loon, A.; Iedema, P.; Chapman, R.; Drennan, J.; Jack, K.; Rasch, R.; Morgan, G.; Zhang, Z.; Monteiro, M.; Keune, K. Electron Microscopy Imaging of Zinc Soaps Nucleation in Oil Paint. *Microsc. Microanal.* **2018**, *24*, 318−322.

(9) van den Berg, J. D. J.; Vermist, N. D.; Carlyle, L.; Holcapek, M.; Boon, J. J. Effects of traditional processing methods of linseed oil on the composition of its triacylglycerols. *J. Sep. Sci.* **2004**, *27*, 181−199.

(10) Raven, L.; Bisschoff, M.; Leeuwestein, M.; Geldof, M.; Hermans, J.; Stols-Witlox, M.; Keune, K. In *Metal Soaps in Art: Conservation and Research*; Casadio, F., Keune, K., Noble, P., van Loon, A., Hendriks, E., Centeno, S., Osmond, G., Eds.; Springer: Cham, Switzerland, 2019; pp 345−357.

(11) Gabrieli, F.; Rosi, F.; Vichi, A.; Cartechini, L.; Pensabene Buemi, L.; Kazarian, S. G.; Miliani, C. Revealing the Nature and Distribution of Metal Carboxylates in Jackson Pollock's Alchemy (1947) by Micro-Attenuated Total Reflection FT-IR Spectroscopic Imaging. *Anal. Chem.* **2017**, *89*, 1283−1289.

(12) Henderson, E. J.; Helwig, K.; Read, S.; Rosendahl, S. M. Infrared chemical mapping of degradation products in cross - sections from paintings and painted objects. *Heritage Sci.* **2019**, *7*, 71.

(13) Casadio, F., Keune, K., Noble, P., van Loon, A., Hendriks, E., Centeno, S., Osmond, G., Eds.; *Metal Soaps in Art: Conservation and Research*; Springer International Publishing: 2019.

(14) Ishioka, T.; Shimizu, M.; Watanabe, I.; Kawauchi, S.; Harada, M. Infrared and XAFS study on internal structural change of ion aggregate in a zinc salt of poly(ethylene-co-methacrylic acid) ionomer on water absorption. *Macromolecules* **2000**, *33*, 2722−2727.

(15) Yano, S.; Nakamura, M.; Kutsumizu, S. Coordination-structural change with pressure around atmospheric pressure in Zn(II) carboxylate salts of ethylene-methacrylic acid copolymer. *Chem. Commun.* **1999**, 1465−1466.

(16) Andor, J. A.; Berkesi, O.; Dreveni, I.; Varga, E. Physical and chemical modification of zinc carboxylate-containing lubricants by molecular structure changes. *Lubr. Sci.* **1999**, *11*, 115−134.

(17) Hermans, J. J.; Baij, L.; Koenis, M.; Keune, K.; Iedema, P. D.; Woutersen, S. 2D-IR spectroscopy for oil paint conservation: Elucidating the water-sensitive structure of zinc carboxylate clusters in ionomers. *Science Advances* **2019**, *5*, No. eaaw3592.

(18) Hermans, J.; Helwig, K. The Identification of Multiple Crystalline Zinc Soap Structures Using Infrared Spectroscopy. *Appl. Spectrosc.* **2020**.

(19) Grady, B. P.; Goossens, J. G. P.; Wouters, M. E. L. Morphology of zinc-neutralized maleated ethylene-propylene copolymer ionomers: Structure of ionic aggregates as studied by X-ray absorption spectroscopy. *Macromolecules* **2004**, *37*, 8585−8591.

(20) Dong, J.; Weiss, R. Shape memory behavior of zinc oleate-filled elastomeric ionomers. *Macromolecules* **2011**, *44*, 8871−8879.

(21) Ikeda, Y.; Yasuda, Y.; Ohashi, T.; Yokohama, H.; Minoda, S.; Kobayashi, H.; Honma, T. Dinuclear bridging bidentate zinc/stearate complex in sulfur cross-linking of rubber. *Macromolecules* **2015**, *48*, 462−475.

(22) Basu, D.; Agasty, A.; Das, A.; Chattopadhyay, S.; Sahu, P.; Heinrich, G. Phase changing stearate ions as active fillers in multifunctional carboxylated acrylonitrile−butadiene composite:

Exploring the role of zinc stearate. *J. Appl. Polym. Sci.* **2020**, *137*, 48271.
(23) Baij, L.; Hermans, J. J.; Keune, K.; Iedema, P. D. Time-Dependent ATR-FTIR Spectroscopic Studies on Solvent Diffusion and Film Swelling in Oil Paint Model Systems. *Macromolecules* **2018**, *51*, 7134−7144.
(24) Di Tullio, V.; Zumbulyadis, N.; Centeno, S. A.; Catalano, J.; Wagner, M.; Dybowski, C. Water Diffusion and Transport in Oil Paints as Studied by Unilateral NMR and 1H High-Resolution MAS-NMR Spectroscopy. *ChemPhysChem* **2020**, *21*, 113−119.
(25) Helwig, K.; Poulin, J.; Corbeil, M.-C.; Moffatt, E.; Duguay, D. In *Issues in Contemporary Oil Paint*; van den Berg, K., Ed.; Springer: 2014; pp 167−184.
(26) Hermans, J.; Keune, K.; van Loon, A.; Iedema, P. The crystallization of metal soaps and fatty acids in oil paint model systems. *Phys. Chem. Chem. Phys.* **2016**, *18*, 10896−10905.
(27) Helwig, K.; Monaghan, M.; Poulin, J.; Henderson, E. J.; Moriarty, M. Rita Letendre's Oil Paintings from the 1960s: The Effect of Artist's Materials on Degradation Phenomena. *Stud. Conserv.* **2020**, 1.
(28) Tumosa, C. S.; Erhardt, D.; Mecklenburg, M. F.; Su, X. Linseed oil paint as ionomer: Synthesis and characterization. *Mater. Res. Soc. Symp. Proc.* **2004**, *852*, 25−31.
(29) Solé, V. A.; Papillon, E.; Cotte, M.; Walter, P.; Susini, J. A multiplatform code for the analysis of energy-dispersive X-ray fluorescence spectra. *Spectrochim. Acta, Part B* **2007**, *62*, 63−68.
(30) Modugno, F.; Di Gianvincenzo, F.; Degano, I.; van der Werf, I. D.; Bonaduce, I.; van den Berg, K. J. On the influence of relative humidity on the oxidation and hydrolysis of fresh and aged oil paints. *Sci. Rep.* **2019**, *9*, 5533.
(31) Soucek, M.; Khattab, T.; Wu, J. Review of autoxidation and driers. *Prog. Org. Coat.* **2012**, *73*, 435−454.
(32) Sturdy, L. F.; Wright, M. S.; Yee, A.; Casadio, F.; Faber, K. T.; Shull, K. R. Effects of zinc oxide filler on the curing and mechanical response of alkyd coatings. *Polymer* **2020**, *191*, 122222.
(33) Barman, S.; Vasudevan, S. Melting of saturated fatty acid zinc soaps. *J. Phys. Chem. B* **2006**, *110*, 22407−22414.
(34) Osmond, G. In *Metal Soaps in Art: Conservation and Research*; Casadio, F., Keune, K., Noble, P., van Loon, A., Hendriks, E., Centeno, S., Osmond, G., Eds.; Springer International Publishing: 2019; pp 25−46.

https://dx.doi.org/10.1021/acsapm.0c00979
ACS Appl. Polym. Mater. 2020, 2, 5674−5685